

Correlative Band Mapping for Multi Spectral Image Fusion

Shaikh Afroz Fatima Muneeruddin, Fabiha Fathima, Sameera Iqbal Muhammad Iqbal

Abstract: This paper presents the process of image fusion, based on spectral correlative property. In the process of image fusion, frequency domain image fusions are more effective in coding compared to spatial domain fusion. In the process of frequency based fusion coding, wavelet approach is used in various formats to obtain spectral resolution and a fusion mapping is derived to map these resolution information. Wherein, spectral based fusion approach has higher significance of image coding accuracy, the resolution code overhead is observed. It is seen that, for larger resolution information's, the retrieved accuracy of fusions higher, however the processing coefficients are large in count. To overcome this processing overhead issue, a new approach based on correlative band mapping approach is proposed. The evaluation result for the proposed approach illustrates a higher accuracy in fusion region prediction and mapping accuracy.

Index term: Image Fusion, Hierarchical Modeling, correlative band mapping approach, wavelet coding.

I. INTRODUCTION

Image fusion has been an area of application in image coding for various usage, such as image representation, resolution enhancement, medical diagnosis, etc. In a image fusion approach, different samples are merged or fused together, either captured from different capturing device of the same scene or samples already registered from a reference source. Such encoding process is of primary importance to handle multiple images in a synchronized manner to achieve the goal of representing the best image. Image coding methods and image fusion have been developed in various approaches. This approach has been developed in two main domains spatial and transformed domain. Different methods have been developed to optimize the quality of the fused image using the converted spatial or space approach to ensure the representation. Among these approaches, spectral domain based coding is more effective in operation. Wherein, the resolution bands are used for representing the image coefficient by successive filtration process of high and low pass filtration. The resolution coding is an optimal approach, however with coding overhead. To achieve the objective of lower coding overhead, in this paper a correlative band mapping approach is suggested. A correlative band selections process is developed to achieve the objective of higher fusion efficiency in image fusion. To present the suggested approach, this paper is outlined in 7 sections.

Manuscript published on 28 February 2019.

*Correspondence Author(s)

Shaikh Afroz Fatima Muneeruddin, Dept. of Computer Science, College of arts and sciences for girls, King Khalid University, Abha, Kingdom of Saudi Arabia.

Fabiha Fathima, Dept. of Information Systems, College of arts and sciences for girls, King Khalid University, Abha, Kingdom of Saudi Arabia

Sameera Iqbal Muhammad Iqbal, Dept. of Computer Science, College of arts and sciences for girls, King Khalid University, Abha, Kingdom of Saudi Arabia

© The Authors. Published by Blue Eyes Intelligence Engineering and Sciences Publication (BEIESP). This is an [open access](https://creativecommons.org/licenses/by-nc-nd/4.0/) article under the CC-BY-NC-ND license <http://creativecommons.org/licenses/by-nc-nd/4.0/>

Section II presents the past developments in the approach of spectral approach to image fusion and its application. Section III outlines the conventional coding of image fusion in wavelet domain. The suggested approach of correlative band mapping approach is outlined in section IV. Obtained experimental results and the conclusion derived from the developed work is outlined in section V, VI respectively.

II. LITERATURE OUTLINE

Toward the approach of image fusion, various past works were developed. In [1] a linking fusion method based on optimal penetration rate was suggested. It was put into a realistic platform for database data and a more appropriate methodology is used to implement a full angle of view. Fused image object of image fusion algorithms for the comparison of different performance evaluations are presented in [2]. Structural similarity ratings that do not use a reference image for image fusion is presented. In [3] A powerful method of investigating multispectral data fusion is proposed for multi-temporal synthetic aperture radar segmentation (SAR), optical data environment for detailed urban data covering. A edge growing and merging algorithm has been developed for the SAR and optical data in fusion model. A precise color array detection method for multi-channel data fusion techniques with different aspects of information based on the gradient in the image have been developed to replicate continuous edges in [4]. Edge is very noise sensitive. Lower pre-filtering algorithms are generally accepted used at very critical levels. A new non-linear pre-filter, image B component of R, G, and is used to reduce noise. Methods edges, corners and subtle image details, protect corrected Gaussian noise and do not require any a priori knowledge. Based on the relationship between ground targets unchanged position between a technical references and recommended a method was proposed in [5], to cover displays matching patterns. This fusion using the wavelet coefficients of a target as well as removing the reference images respectively paired control points (CP) and the detected search routine comprises a geometric mapping rating. Multimodal brain imaging for certain clinical applications is outlined in [6]. Usually PET images MR image shows the anatomy of the brain and includes functional data shows the brain function and have low spatial resolution. Therefore, no color distortion and spatial information includes the functional and spatial characteristics are presented as well as an excellent molten image. For much focused image fusion [7] A new discrete wavelet transform (DWT) based approach is presented. Method was developed by identifying a separate low frequency and consistency verification process followed different rules for high-frequency sub-band components.

In this way, the minimum free frequency domain is used for the selection of the coefficients of high frequency sub-band coefficients for maximum free frequencies is outlined in [8]. In this technique, MS image PC conversion of principal components (PC) has been proposed to achieve. [9] Neural Networks (PNN) Coupled Contourlet associated with a lower impact Non-sampled (NSCT) Contourlet Transform Shift-invariant transform to come from the missing handle. In this case the original image is separated to obtain sub-band coefficients of the modified PCNN. The original images and the spatial frequency fusion rule matching degree is determined and are used, respectively. In [10], it has been proposed advanced ICE fusion method. There are two main aspects of the improvements. First, an appropriate way to measure they are using entropy IC gauss, the main body of the individual components (MBIC) are presented to select; secondly, direct panchromatic (PAN) to avoid too spatial information MBIC caused by changing the image is applied to obtain detailed information of the image of a wavelet decomposition Pan. In order to be completed by different images in different situations, different fusion techniques used to ensure the completion of the image [11]. Various resolution based image coding have been suggested in the Fusion format and Image Fusion Algorithm following a Low root mean Square Error (RMSE) outlined in [12], based on the average. As has been carried out on the center-resolution image fusion model [13] based on a comparative study of the images and TM MODIS data. Fusion unsupervised classification of the original image and two images (PC and HIS) was used on respectively. Land area change and the rate of change calculated and had different data fusion models discoloration effect. A Discrete wavelet transformation (DWT) and a new image fusion incorporating a discrete Ripplet (SET) transformation were illustrated in [14]. DWT initially converted to images using multi-resolution image. More images converted using the DRT approach. Ripplet coefficients Neural Network (PCNN) Coupled pulse is applied and fire maps are produced. Maximum fusion rules and fused coefficients obtained by applying the reverse image of the DRT approach. discrete Ripplet (DRT) was defined for image fusion algorithm in [15]. The Intersecting Cortical Model (ICM) remote control is used to create a better decision to get all the sub-band fusion advantages. A scalable tile-based frame work of merging all about image processing is presented in [16], while providing the same results, part of large images algorithms. The benefits shown in this frame and is scalability of this approach was carried out by applying a real great footage. In the adaptive wavelet-based framework [17] to the local geometric structure of a new medical image fusion method is shown. Local image structure of the core values and structure tensor Eigen values for each image is described. The area based multi-sensor image fusion approach has been proposed in [18]. Here a 3×3 filter mask is applied to the first stage of input data. A watershed algorithm based on the marker derived from the input images is divided into segments that show similar computing devices. Thereafter, a pixel area was added to calculate the relative importance of the area. Direction has been proposed based on a novel fusion algorithm and turn it into fusion rate [19] indicated a hoist with improved efficiently by transforming cotton. Transformation of the direction and the alignment direction of this approach was decomposed with direction by removing two proprietary

source images. [20] Explores the possibility of using the wavelet image fusion and denoising specialist approach. Approach followed by an affine transformation uses wavelet-based image fusion record. Based on least squares support vector machines for image denoising works to reduce the frequency band selection is proposed. Notches works to reduce image blur and the ultimate super, resolution is to remove the top level. The two-stage solid pedestrian detection approach [22] was outlined. The first stage uses a single image is applied to a full-body detector to create a pedestrian island. In the second stage, the detector is confirmed by a community consisting of all pedestrian part of the island detectors. As part detector features to benefit the Haar wavelet-like full-body detector is trained by the improved shape features. The conventional fusion approaches were observed to perform well under transformed domain. In the work, the transformed approach is used based on DWT, to fusion process.

III. WAVELET IMAGE FUSION

In the process of image coding, captured images are processed for image enhancing. In the pre process operation, the image are filtered using a adaptive histogram equalization (AHE) using a recursive regularized filter (RRF) [21]. A weight factor updation is used in the approach of denoising and sharpening of color information. The enhanced image optimize the color and contrast updation. The streaming map approach is used as a a measure of artifact removal in the image. In the presentation towards image fusion in [5] wavelet spectral representation of image bands is presented. A voting method for predicting the image fusion segments, based on the correlation approach to extract control point by searching of wavelet coefficient fusion. In the approach of wavelet based image fusion the bands are decomposed using successive filter hierarchy. For the process of image fusion, the obtained band coefficients are considered as a coefficient, derived from an information point. According to the statistical approach, the weight bit of the source data probability distribution I used. Shannon-based approach, process on coefficient for one symbol (S) information in the image data and the content is measured by its entropy:

$$H = -\text{Log}_2 P_b \quad (1)$$

Where P_b is defined as the probability of occurrence.

The Entropy of the entire image can then be derived as average entropy of all pixels:

$$H_{image} = -\frac{1}{n} \sum_{i=1}^n \text{Log}_2 P_{b_i} \quad (2)$$

Here, P_{b_i} is defined as the pixel probability and the total pixel count us given by 'n'.

Source alphabet (black and white pixels) is known in priori, and the probability distributions, the probability model is then defined by the entropy expressed as:

$$H = -P_{bw} \text{Log}_2 p_w - P_B \text{Log}_2 p_B \quad (3)$$

Where P_{bw} and P_B are the white and black pixels possibilities respectively.

Form geometric structures with appropriate spatial dependence of pixels in the image. dependence can be described with a limited and localized neighborhood-based hierarchical statistical model.



In this model, the probability is defined as apparent pixel black-and-white configuration of neighboring pixels in the local template hierarchical C, depending on the circumstances. For binary images, black pixels probability (N_B^C) is calculated by counting white (N_W^C) appearing in all pixels displayed as hierarchical output:

Here, P_B^C , P_{bW}^C , are from black and white pixels. Hierarchical 'C' entropy H(C) for all the pixels in the hierarchy is defined as the average entropy defined by:

$$p(x) = \begin{cases} P_{bW}^C = \frac{n_W^C}{n_W^C + n_B^C}, & \text{if } x = \text{White} \\ P_B^C = 1 - P_{bW}^C, & \text{if } x = \text{black} \end{cases} \quad (4)$$

$$H(C) = -p_{bW}^C \log_2 p_{bW}^C - p_B^C \log_2 P_B^C \quad (5)$$

A band of small entropy has skewed distributions and therefore has a smaller information content. N-level band model entropy is the weighted sum of the individual bands given by,

$$H_N = -\sum_{j=1}^N p(C_j) \cdot (p_{bW}^{C_j} \cdot \log_2 p_{bW}^{C_j} + p_B^{C_j} \cdot \log_2 p_B^{C_j}) \quad (6)$$

In principle, the skewed distribution can be achieved using larger band pattern through tuning of large band templates. However, in this way, entropy increases the cost of modeling and result in offset model. The statistical model suggests a large number of parameters, thus affecting the accuracy of the count statistics and probability estimates, when distributed over a large number of resulting bands, which result in "band dilution" problem. This problem raises the issue of processing overhead. To mitigate the issue a correlative band mapping is proposed.

IV. CORRELATIVE BAND MAPPING

Accuracy of the estimate or learning costs are a trade-off between model overhead and processing band size. The larger size of the template gives better theoretical prediction accuracy. This results in improvement of probability distribution, and low bit-rates. To create a group of trees, image is processed and statistics, including n_W^1 and n_B^1 for internal nodes are calculated for each group in a full tree. Children and parent nodes at all levels of the tree are pruned after comparing each node. Using the fusion gain children node are linked to the parent node's, or removed children from their parent tree to become a leaf node. The fusion gain is defined by;

$$\text{Gain}(C, C_W, C_B) = l(C) - l(C_W) - l(C_B) - \text{Split Cost}, \quad (6)$$

Where C is parent band and C_W and C_B are two children bands. Coding is encoded using the length of the L-band pixel output showing the total number of processing bits. Cost split buffer the tree storing cost. The occurrence of the pixel is computed as the entropy code given by,

$$l(C) = \sum_t \log p^t(C) \quad (7)$$

Here each pixel coefficient is computed by the Bayes probability given by,

$$p^t(C) = \begin{cases} P_{bW}^t(C) = \frac{n_{bW}^t(C) + \delta}{n_{bW}^t(C) + n_B^t(C) + 2\delta}, & \text{if } t^{\text{th}} \text{ pixel is White} \\ P_B^t(C) = 1 - P_{bW}^t(C), & \text{if } t^{\text{th}} \text{ pixel is black} \end{cases} \quad (8)$$

Where P_{bW}^t, P_B^t where the possibilities for white and black colors, and n_{bW}^t, n_B^t is time-dependent frequencies. The value of δ is taken to 0.45. The signal processing of the different decomposed bands is used to attempt for achieving high level accuracy in image processing applications. In the band's representation, information is revealed using finer bands processing over the original signal. However, the decomposed band increases the probability of redundancy between different bands. This information increases the additional processing data and the processing speed is decreased. Therefore, an appropriate band selection procedure is required to extract the original Information. In this work, band selection process with reference adaptive band selection process has been developed for multi wavelet coefficients. Figure 1 shows, a process of transformation for analysis and synthesis filter, showing band decomposition operation,

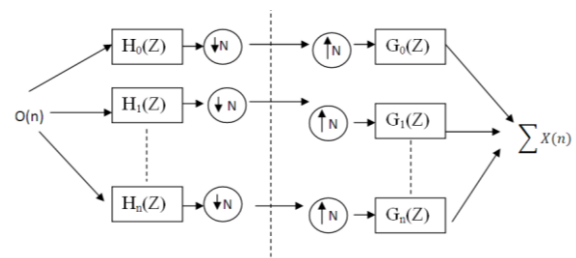


Figure.1. Analysis and synthesis branch of an n-channel filter bank

In this process K sub bands are generated with analysis branch $H_z(k)$ generating each image I into different fragments. After a decimation factor N and expansion, the full band signal is the sum of filters $G_k(z)$ obtained by the synthesis filter bank, reconstructed from the sub-bands. The analysis $H_k(n)$ is obtained from the low pass filter $p[n]$ of even length L_p . In the sub-band adaptive filters process is used where cost optimization approach to calculate the signal with the use of the DWT using the LMS-type adaptive filter. The combined factor of filtering function with weight factor is used to optimize an average error based on LMS function optimization. The default-state error convergence rate increases when the function is added to this function more quickly, increasing the sub-band filter count. A Dynamic Selection is proposed to overcome this problem. The approach in this approach is a subset of sub-band filters that work in conjunction with the performance and use the adaptive filter to weigh the correlative weights among the bands. A recursive mean Square deviation (MSD) is used for dynamically choosing sub-band filters to achieve convergence problem. This approach also reduces the complexity of the traditional Computing using critical sampling operation.

For a conventional DWT coding, the received signal is defined by,

$$d(n) = u(n)W^o + v(n) \quad (9)$$

wherein the unknown vector $v(n)$ is predicted detecting w^o for the variance σ_v^2 respectively. For each band $B(n)$, defined with a length representing a input vector with length M , given by,

$$B(n) = [B(n) B(n - 1) \dots B(n - M + 1)] \quad (10)$$

For the estimation of band selection process a adaptive selection architecture is proposed, as shown Figure 2,

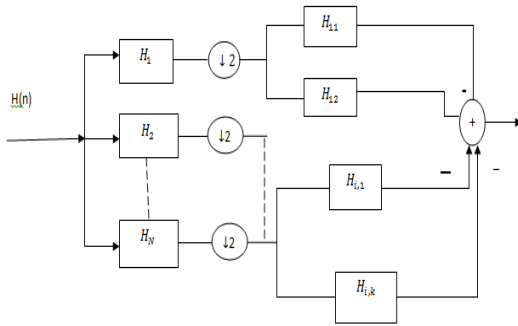


Figure 2. NDWT filter architecture

For the Analysis filter defined by, $H_0(z), \dots H_{n-1}(z)$ filter, the image is divided into K sub-bands. The resulting sub-band signals are then decimated to meet the demand for bandwidth at a lower sampling rate. For a original signal $O(n)$, the resulting band decomposition $y_{i,D}(k)$ is defined as the decimated filter output;

$$y_{i,D}(k) = B_i(k)w(k), \quad (11)$$

Where, $B_i(k)$ is a $1 \times M$ coefficient of the band given by,

$$B_i(k) = [B_i(kN), B_i(kN - 1), \dots, B_i(kN - M + 1)]$$

and,

$$w(k) = [w_0(k), w_1(k), \dots, w_{M-1}(k)]^T$$

defines the estimated weight and the band error is given by,

$$be_{i,D}(k) = O_{i,D}(k) - y_{i,D}(k) = O_{i,D}(k) - B_i(k)w(k) \quad (12)$$

Here $O_{i,D}(k) = O_i(kN)$ are each band reference information. In the NDWT process a weight control process is used, given by,

$$w(k + 1) = w(k) + \mu \sum_{i=0}^{N-1} \frac{B_i^T(k)}{\|B_i(k)\|^2} be_{i,D}(k) \quad (13)$$

μ is given step value $\in 0.1$.

the optimization convergence calculation takes a large computation to optimize the selection process. A MSD-based weight optimization is proposed to overcome this problem. This approach is used by a large variation in the MSDs between two successive iterations. Its weight error vector is then, defined as $\tilde{w}(k) = w^o - w(k)$. On optimization of the weight is then defined as,

$$\tilde{w}(k + 1) = \tilde{w}(k) - \mu \sum_{i=0}^{N-1} \frac{B_i^T(k)}{\|B_i(k)\|^2} be_{i,D}(k) \quad (14)$$

This weight is calculated by the vector and is expected to be an MSD, since it is quite anticipated, along with the overall expectation of satisfying the required expectations with the constraint of ,

$$E \|\tilde{w}(k + 1)\|^2 = E \|\tilde{w}(k)\|^2 + \mu^2 E \left[\sum_{i=0}^{N-1} \frac{be_{i,d}^2(k)}{\|B_i(k)\|^2} \right] - 2\mu E \left[\sum_{i=0}^{N-1} \frac{B_i(k)\tilde{w}(k)be_{i,D}(k)}{\|B_i(k)\|^2} \right] \triangleq E \|\tilde{w}(k)\|^2 \quad (15)$$

Where

$$\Delta = \mu \sum_{i=0}^{N-1} \left(2E \left[\frac{B_i(k)\tilde{w}(k)be_{i,D}(k)}{\|B_i(k)\|^2} \right] - \mu E \left[\frac{be_{i,d}^2(k)}{\|B_i(k)\|^2} \right] \right) \quad (16)$$

Gives the correlation of two consecutive bands MSD's. The lowest MSD bands are selected after the successive correlation process. This is due to the band selection process of selecting the minimum value MSD, which reduces the processing coefficient with minimal deviation from the convergence criteria.

V. EXPERIMENTAL RESULTS

To evaluate the proposed approach, for color image fusion simulation was developed to evaluate the modeling of spatial map images. These images are high contrast colored and contain large textural Variations. A System architecture for fusion is designed for such image is as illustrated.

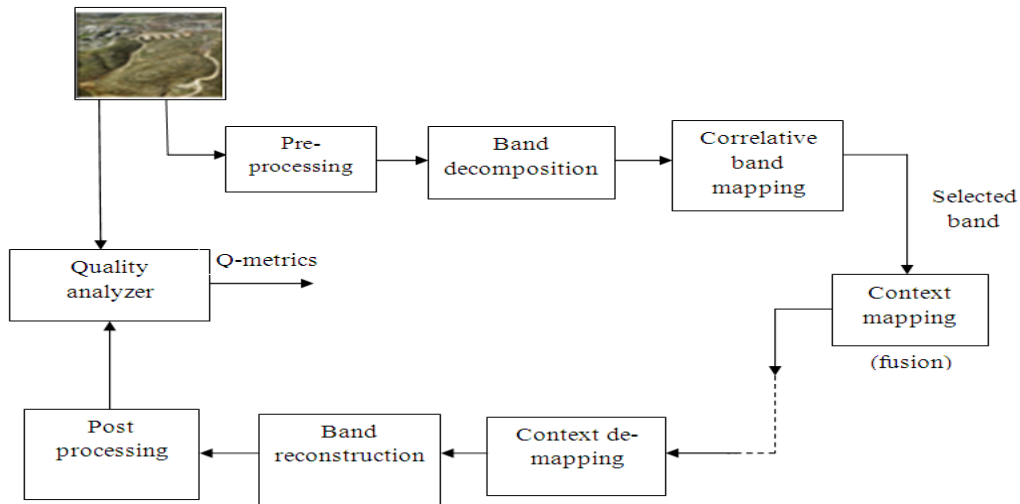


Figure 3. Architecture for the proposed fusion model

This system, process on gray color image data, read from the original colored sample. During pre-processing, image is made to uniform level to normalize the intensity distribution made with histogram equalization is process. The equalized image is then processed to estimate the region of interest, by using Bi-thresholding technique. Operation that applies mathematical morphology to extract map flanking regions and curves in the image. Tree modeling is then developed for the extracted region to obtain a feature region. A tree model as described in previous sections considering band feature were developed. Context considerably reduced the number of features needed for the fusion objective. A pruning is then done to achieve lower band coefficients. By the pruning, hierarchical tree is traced to reduce the size of a watch band features using hierarchical coding technique. The obtained coefficients are presented in comparison to reduce, discarding intermediate band characteristics. This pruning process results in mapping information resulting dominant band features with minimum number of band selected. This image feature is used for entropy coding which results in faster computation. The band coefficients are mapped by pruning out and created a map showing the binary stream data. This flow of entropy coding using Huffman entropy encoder is passed to perform binary fusion. The Quantized information is passed for the demapping operation. The image is taken with coefficients of quantized data to obtain information of the original image information back. Demapping operation as actuated by reference band table mapping is performed in a similar manner. The same band index coefficients for pixels are used for the regeneration of the inverted tree created to get the pixel coefficients. After the coefficients obtained is processed to form the final image. This unit aligns pixel grid according to the coefficient index band formed during pre-processing. After calculating the predicted accuracy of the received image quality factor for the performance evaluation of the proposed architecture PSNR value is evaluated. A Spatial image for the processing of a developed system is passed in color format. In order to ensure the highest accuracy through images a higher resolution data to obtain the best extraction group is processed. The system reads out the original sample and passes to the normalization and for further processing to compute the histogram taken in a spectral domain to formulate the distribution plot. The Histogram for the given query sample is shown below.



Figure 4: Original Test Image

Figure 4 illustrates the original test sample taken for the evaluation. The image is taken in RGB color format, with different terrestrial information's, illustrating as variations. The test sample is then pre-processed, where the given test sample is scaled to a uniform dimension of 256 x 300 dimensions, and the gray pixel content is extracted. For the deriving of control points for fusion, a histogram based spectral energy computation is made. The obtained spectral histogram is shown in figure 2.

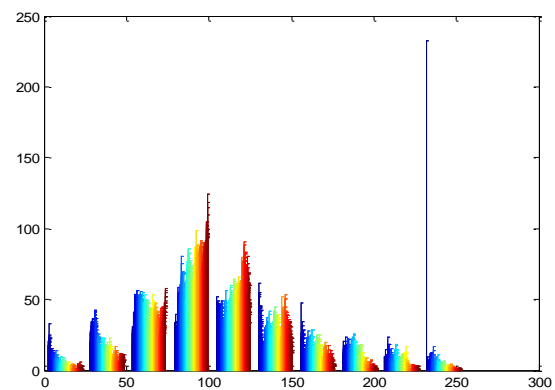


Figure 5. Histogram plot for the given query Sample

The Obtained Histogram is used for the equalization of variation developed due to capturing intensity effect or surrounding effects. The obtained equalized result is shown in figure 6.



Figure: 6. Equalization on the test sample

The energy distribution of this image is then used to pick the first level region of interest. With higher energy density. The coefficients with large energy values are then selected. These coefficients are used as a marking bounding region for region extraction. For the extraction of region of interest, a binarized thresholding is used.

Binary implementation using an advanced approach that uses the image areas to distinguish objects or background is presented. Locating for a terrestrial or non-terrestrial region in the test image. This method separates the system of the fact that the intensity of the terrestrial surface is greater than that of the non-terrestrial region. So an appropriate limit for the distinction of terrestrial and non-terrestrial region is evaluated. The method Calculates the dynamic threshold value 'K' as a target value. Each pixel of the image is processed to get the threshold value of the target through its neighboring pixels. Two mask operators use mask compatibility to calculate the value of threshold. For the given image, 'I' the threshold 'K' is given by,

$$K = \frac{\sum_{i=1}^m \sum_{j=1}^n I(i,j) \times m(i,j)}{\sum_{i=1}^m \sum_{j=1}^n m(i,j)} \quad (17)$$

Where,

$$m(i,j) = \text{Max}(|F1 \oslash I(i,j)|, |F2 \oslash I(i,j)|) \quad (18)$$

and,

$$F1 = [-1 \ 0 \ 1], \quad F2 = F1^t \quad (19)$$

In Eqn. 18, " \oslash " denote two-dimensional linear convolution. Using Eqn. 17 threshold 'K' is used to transform to a two level logic given by,

$$e(i,j) = \begin{cases} 1, & \text{if } es(i,j) > K \\ 0, & \text{otherwise.} \end{cases} \quad (20)$$

The obtained binarized sample for the processed image is illustrated in figure 7.



Figure: 7. Region Extraction via Bi-thresholding

The result shows the detected region of interest, where the non-homogenous pixel distribution is considered for the region extraction. The urban region is more accurately been

highlighted, due to the dynamic thresholding, as the threshold is derived from the image with maximum neighbor pixel distance. This extracted region is processed with wavelet coding to define the finer spectral bands. These spectral bands are coded with proposed correlative approach, for selecting the fusion control point. The selected band from the correlative process is illustrated in figure 8(a),(b).



(a)



(b)

Figure: 8. Operative bands selected (a) Diagonal-Band (b) Approximate-Band

The derived control point for the processed sample is shown in figure 9. The extracted control points illustrates the distinct points of representation. The CP point is used for selecting the image coefficient for fusion without much of information loss.

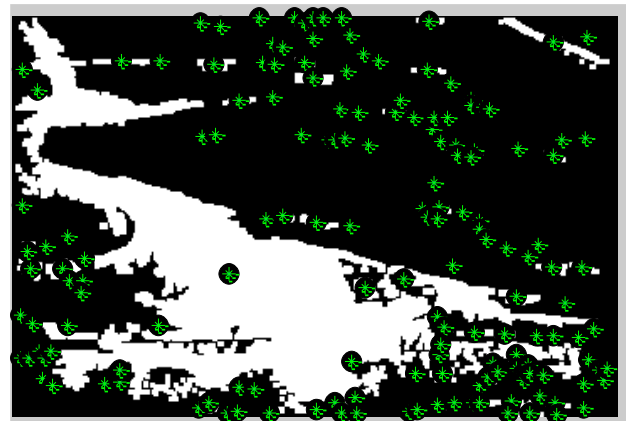


Figure: 9. Extracted control point



Figure: 10. Image fusion result

The quantitative analysis of the proposed approach is carried out. The obtained result for the system is as shown below.

Three measures for the evaluation of the proposed work is made, namely, SSIM, Computation time (CT) and Root Mean Square error (RMSE). The SSIM factor defined the structural similarity in retrieval before and after fusion. This factor is given by,

$$SSIM = \frac{\sum_i \sum_j f(i,j) \otimes f_w(i,j)}{\sum_i \sum_j (f(i,j))^2} \quad (21)$$

The evaluation of the proposed approach is carried out on different dimension test image. Different dimension of, 64 x 64, 128x128, 256 x 256 and 512 x 512 is taken. The evaluation is also performed at different level of bit depth of pixel per image.

The RMSE factor is defined as,

$$RMSE = \sqrt{MSE} \quad (22)$$

The mean square error (MSE) of a the image is a defined as an estimate of difference from the actual value to the estimated one. MSE calculates the average error of the original over retrieved image. The error is defined as a difference of the estimation error given by,

$$MSE = \frac{1}{M \times N} \sum (I - \hat{I})^2 \quad (23)$$

Here, I is the original image and \hat{I} is the computed image result. The observation for the developed approach is illustrated as,

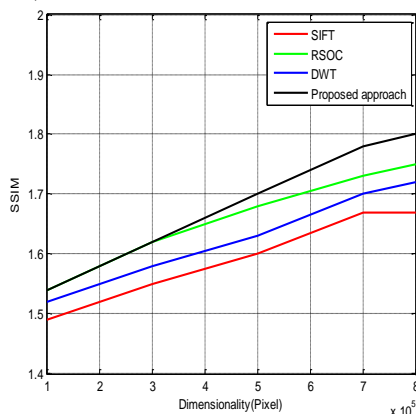


Figure 11. Observed SSIM over dimensionality variation of test Image

The observed SSIM for the developed method is compared with the conventional methods of Discrete wavelet transform (DWT) based coding, and scale-invariant feature transform (SIFT), restricted spatial order constraints (RSOC) method. The SSIM factor for the developed approach is about 0.08- 0.1% higher than the comparative approaches. The Root mean square for the developed approach is shown in figure 12. The Obtained RMSE is about 0.2% lower than the conventional approaches.

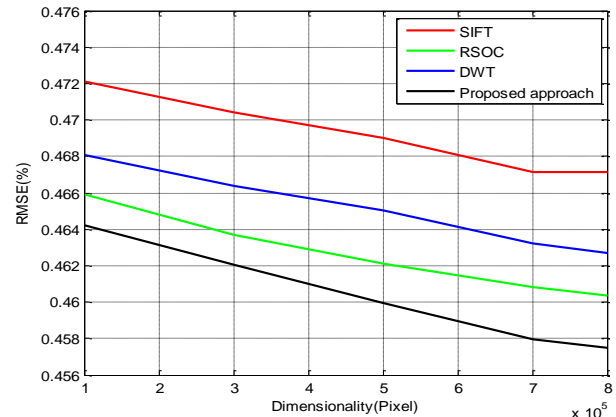


Figure 12. Observed RMSE over dimensionality variation of test Image

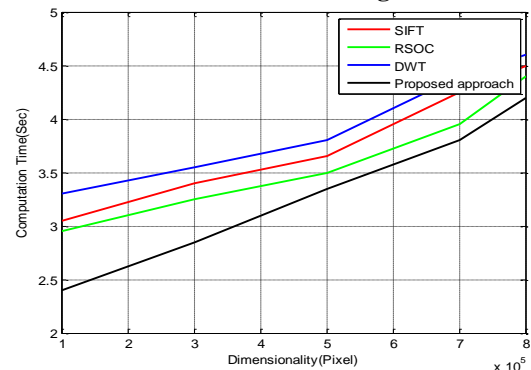


Figure 13. Observed Computation time over dimensionality variation of test Image

The computation time is measured as the total time taken to process the test image with CP detection, band selection and fusion process. The time taken get increase with the dimensional increment. However, the time taken to process is lower as in comparison to conventional model due to lower CP values. The developed approach is also evaluated with the variation in bit depth factor of the test image. The obtained results are as shown below,

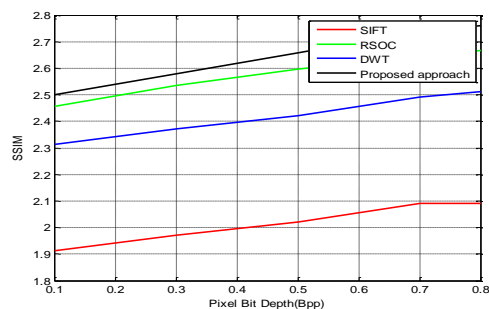


Figure 14. Observed SSIM over Bpp variation of test Image

Correlative Band Mapping For Multi Spectral Image Fusion

In 8-bit depth graph at low bit level fusion is high for the band tree method because it is a hierarchical band tree where as existing has very low fusion but for higher bit depth, the suggested the proposed approach reach to a higher SSIM factor. The RMSE and the observed computation time are illustrated in figure 15 and 16, respectively.

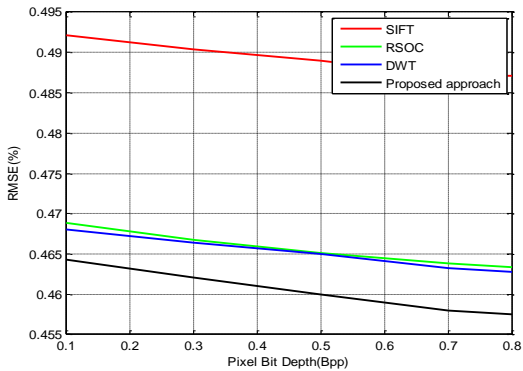


Figure 15. Observed RMSE over Bpp variation of test Image

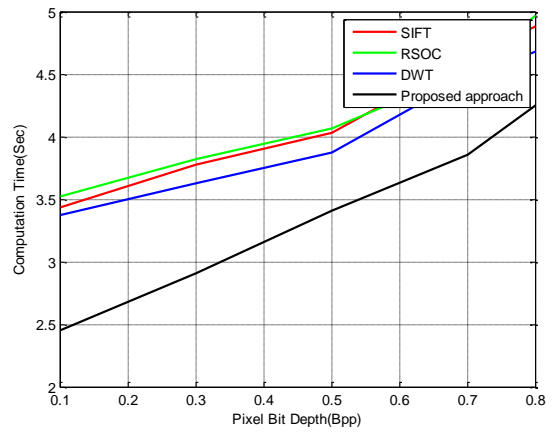


Figure 16. Observed CT over Bpp variation of test Image

The process is repeated for different test samples, and the observations are summarized in Table 1, 2.

Sample	Dimension	SIFT approach			RSOC			DWT			Proposed approach		
		SSIM (%)	RMSE (%)	CT (sec)	SSIM (%)	RMSE (%)	CT (sec)	SSIM (%)	RMSE (%)	CT (sec)	SSIM (%)	RMSE (%)	CT (sec)
S1	64 x 64	1.3	0.43	2.5	1.6	0.42	2.4	1.7	0.44	2.53	1.9	0.41	2.1
	256 x 256	2.2	0.46	3.3	2.4	0.44	3.6	2.6	0.45	3.4	2.9	0.42	3.2
	512 x 512	2.5	0.49	3.9	2.8	0.47	3.2	2.9	0.49	3.7	3.1	0.45	3.5
S2	64 x 64	1.6	0.41	2.9	1.2	0.43	2.4	1.3	0.45	2.2	1.5	0.42	2.5
	256 x 256	2.7	0.43	3.1	2.4	0.46	3.3	2.7	0.47	3.4	2.9	0.41	3
	512 x 512	2.9	0.44	3.8	2.7	0.48	3.56	2.9	0.48	3.3	3.2	0.38	3.5
S3	64 x 64	1.3	0.4	2.2	1.1	0.42	2.7	1.3	0.44	2.6	1.5	0.42	2.1
	256 x 256	2.4	0.45	3.5	2.3	0.46	3.8	2.5	0.47	3.8	2.8	0.4	3.3
	512 x 512	2.8	0.463	3.7	2.9	0.47	3.2	2.9	0.49	3.0	3	0.38	3.5

Table 1: Observation for test samples at 8 bit depth per pixel.

Sample	Dimension	SIFT approach			RSOC			DWT			Proposed approach		
		SSIM (%)	RMSE (%)	CT (sec)	SSIM (%)	RMSE (%)	CT (sec)	SSIM (%)	RMSE (%)	CT (sec)	SSIM (%)	RMSE (%)	CT (sec)
S1	64 x 64	1.3	0.46	3.3	1.4	0.47	3.5	1.7	0.44	3.7	1.9	0.41	3.3
	256 x 256	2.3	0.44	3.8	2.43	0.43	3.9	2.6	0.41	4	2.8	0.4	3.7
	512 x 512	2.4	0.47	4.1	2.7	0.46	4.3	2.9	0.44	4.3	3.2	0.41	4.2
S2	64 x 64	1.4	0.42	3.3	1.5	0.44	3.5	1.6	0.43	3.2	1.8	0.42	3.1
	256 x 256	2.3	0.47	3.5	2.6	0.45	3.8	2.8	0.42	3.9	3	0.41	3.3
	512 x 512	2.2	0.49	4.2	2.4	0.45	4.6	2.6	0.42	4.8	2.8	0.4	4.5
S3	64 x 64	1.3	0.41	2.3	1.4	0.43	2.6	1.6	0.41	2.78	1.9	0.4	2.5
	256 x 256	2.5	0.43	3.8	2.6	0.45	3.9	2.8	0.42	4	3.1	0.41	4.3
	512 x 512	2.6	0.44	3.11	2.8	0.47	4	2.9	0.45	4.2	3	0.42	4.8

Table 2: Observation for test samples at 16 bit depth per pixel.

VI.CONCLUSION

A method for image fusion based on correlative property of band coefficient is proposed. The suggested approach of correlative band mapping, results in lesser number of processing bands, which leads to lower processing overhead, as compared to conventional wavelet based coding approach. The developed band tree modeling is focused with the objective of attaining minimum error and faster computations in processing these mapping images for real time applications. The comparative analysis of the developed system, shows a improvement in observe SSIM over the conventional approaches. The RMSE value is reduced for the developed approach. The computation time minimized due to lower bit selection for fusion. The overhead wrt. Processing bit is reduced by band selection, hence the computation time is saved with improvement in quality metric for image fusion operation.

REFERENCES

1. M. Canaud, A.Nabavi, C.Becarie, D.Villegas and N-E El Faouzi,, "A realistic case study for comparison of data fusion and assimilation on an urban network – The Archipel Platform", Transportation Research Procedia Vol.6, pp.28-49, Elsevier, 2015.
2. Zheng Youzhi, Qin Zheng, "Objective Image Fusion Quality Evaluation Using Structural Similarity", Tsinghua Science and Technology, Vol.14, No.6, pp.703-709, IEEE, 2009.
3. Yifang Ban, and Alexander Jacob, "Object-Based Fusion of Multitemporal Multiangle ENVISAT ASAR and HJ-1B Multispectral Data for Urban Land-Cover Mapping", IEEE Transactions on Geoscience and Remote Sensing, Vol. 51, No. 4, IEEE, 2013.
4. Yang Oua, Dai GuangZhia, "Color Edge Detection Based on Data Fusion Technology in Presence of Gaussian Noise", Procedia Engineering, Vol.15, Pp.2439-2443, Elsevier, 2011.
5. Li Dapeng, "A novel method for multi-angle SAR image matching", Chinese Journal of Aeronautics, Vol.28, pp. 240-249 Elsevier, 2015.
6. Changtao He, Quanxi Liu, Hongliang Li, Haixu Wang, "Multimodal medical image fusion based on IHS and PCA", Procedia Engineering, Vol.7, pp.280-285 Elsevier, 2010.
7. Yong Yang, "A Novel DWT Based Multi-focus Image Fusion Method", Procedia Engineering, Vol.24, pp.177-181, Elsevier, 24, 2011.
8. QifanWanga, ZhenhongJiaa, XizhongQina, JieYangb, YingjieHuc, "A New Technique for Multispectral and Panchromatic ImageFusion", Vol.24, pp. 182-186, Elsevier, 2011.
9. LIU Fu, LI Jin, Huang Caiyun, "Image Fusion Algorithm Based on Simplified PCNN in Non-sub-sampled Contour let Transform Domain", Vol.29, 1434-1438, Elsevier, 2012
10. Fengrui Chena, Fen Qina, GuangxiongPengb, Shiqiang Chena, "Fusion of Remote Sensing Images Using Improved ICA Mergers Based on Wavelet Decomposition", Vol.29, Pp. 2938-2943, Elsevier, 2012.
11. Youdong Ding, Cai xi, Xiao Cheng Wei, Jianfei Zhang, "A New Framework for Image Completion Based on ImageFusion Technology", Vol.29, Pages 3826-3830, Elsevier, 2012.
12. Tao Wu, Xiao-Jun Wu, Xiao-Qing Luo, "A Study on Fusion of Different Resolution Images", Vol.29, pp. 3980-3985, Elsevier, 2012.
13. LU Heli, QIN Yaochen, ZHANG Lijun, LU Chaojun, LU Fengxian, "A Case Study of Model-Based Satellite Image Fusion", Vol.37, pp. 268-273, Elsevier, 2012.
14. C.T.Kavitha, C.Chellamuthu, R.Rajesh, "Medical image fusion using combined discrete wavelet and ripplelet transforms", Vol.38,pp. 813-820, Elsevier, 2012.
15. C.T.Kavitha, C.Chellamuthu, R.Rajesh, "Multimodel medical image fusion using discrete ripplelet transform and intersecting cortical model", Vol.38, pp. 1409-1414, Elsevier, 2012.
16. Pierre Lassalle, JordiInglada, Julien Michel, "A Scalable Tile-Based Framework forRegion-Merging Segmentation", IEEE Transactions on Geoscience and Remote Sensing, Vol.53, pp. 5473 - 5485, IEEE, 2015.
17. Bibo Lu, Hui Wang, Chunli Miao, "Medical Image Fusion with Adaptive Local Geometrical Structure and Wavelet Transform", Vol.8, pp. 262-269, Elsevier, 2011.
18. Sourav Pramanik, Swagati kaPrusty, Debotosh Bhattacharjee , Piyush Kanti Bhunre, "A Region-to-Pixel Based Multi-sensor Image Fusion", Vol.10, pp. 654-662, Elsevier, 2013.
19. Deng Minghua,Zeng Qingshuanga and Zhang Lanying, "Research on Fusion of Infrared and Visible Images Based on Direction let Transform", Vol.3, pp. 67-72, Elsevier, 2012.
20. A. AnoopSuraj, Mathew Francis, T.S. Kavya, T.M. Nirmal, "Discrete wavelet transform based image fusion and de-noising in FPGA", Vol.1, pp. 72-81, Elsevier, 2014.
21. Shaikh Afroz Fatima Muneeruddin, "Visual Improvements in Color Image Processing Using Regularized Filtration", American International Journal of Research in Science, Technology, Engineering & Mathematics, 10(3), March-May, 2015, pp. 277-283
22. Wentao Yao, Zhidong Deng, "A Robust Pedestrian Detection Approach Based on Shape let Feature and Haar Detector Ensembles", Tsinghua Science and Technology, Vol.13 pp. 314-322, IEEE, 2012.